The Microwave Spectrum of 2,6-Lutidine, Analysis of Internal Rotation and ^{14}N Hyperfine Structure

C. Thomsen and H. Dreizler

Abteilung Chemische Physik im Institut für Physikalische Chemie
der Christian-Albrechts-Universität Kiel, 24098 Kiel, FRG

Z. Naturforsch. **48a**, 1093–1101 (1993); received August 11, 1993

The rotational spectrum of 2,6-lutidine, $(CH_3)_2C_5H_3N$, has been recorded between 6 and 26.5 GHz using pulsed molecular beam microwave Fourier transform spectroscopy. The rotational constants are $A = 3509.7139(84)$ MHz, $B = 1906.8639(101)$ MHz, and $C = 1254.6215(14)$ MHz, the barrier to internal rotation of the two methyl groups is $V_3 = 1.1752$ kJ/mol, their moments of inertia were found to be $I_\alpha = 3.0808(9)$ uÅ^2. The nitrogen nuclear quadrupole constants are $\chi_{aa} = +1.600(5)$ MHz, $\chi_{bb} = -4.572(3)$ MHz and $\chi_{cc} = +2.972(5)$ MHz.

Introduction

2,6-Lutidine (LUT), $(CH_3)_2C_5H_3N$ (Fig. 1), is a molecule with two methyl tops and a relative low barrier to internal rotation. The rotorsional levels can be classified under the invariance group $C_{3v}^- \otimes C_{3v}^+$. Its microwave spectrum has been studied for the first time by Caminati and Di Bernardo [1]. They intended to determine the V_3 barrier to internal rotation from the inertial defect of the A_1A_1 torsional sublevels. Erroneously they assigned the measured EE state rotational transitions as A_1A_1 state lines. Consequently the rotational constants and the resulting V_3 barrier were not correct. We were able to measure the A_1A_1, A_1E, EA_1, and the EE state components of several rotational transitions. So we could determine V_3 from the inertial defect of the rotational spectrum in the A_1A_1 state and from the $A_1A_1-A_1E$, $A_1A_1-EA_1$, and A_1A_1-EE splittings. Finally we calculated the nitrogen quadrupole coupling constants from the hyperfine structure of the rotational lines.

Experimental Details

The spectra were recorded using a molecular beam microwave Fourier transform (MB-MWFT) spectrometer. The vacuum chamber is realized as a stainless steel cylinder with a diameter of 400 mm and a length of 600 mm. The mirrors of the Fabry Perot resonator have a diameter of 250 mm and a radius of curvature of 300 mm. The nozzle is mounted near the center of one mirror, with the beam axis parallel to the mirror axis. With this technique the lines appear as Doppler doublets (Fig. 2), with a separation of the Doppler components of 29 kHz at 7.0 GHz to 112 kHz at 26.3 GHz – corresponding to a particle velocity of 624 m/s and a linewidth of approximately 7 kHz (FWHH). The free induction decay was downconverted to an intermediate frequency centered at 10 MHz and was sampled at 8 k points, with an inter-

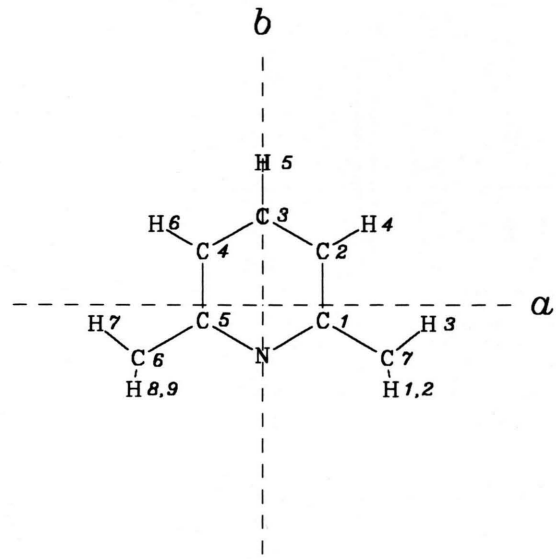

Fig. 1. 2,6-lutidine in its principal inertia axes system (*a*, *b*). The structural parameters are calculated with Gaussian-90 with the basis set 6-311G**.

Reprint requests to Prof. Dr. H. Dreizler, Abteilung Chemische Physik, Institut für Physikalische Chemie, Universität Kiel, Olshausenstraße 40–60, 24098 Kiel FRG.

0932-0784 / 93 / 1100-1093 $ 01.30/0. – Please order a reprint rather than making your own copy.

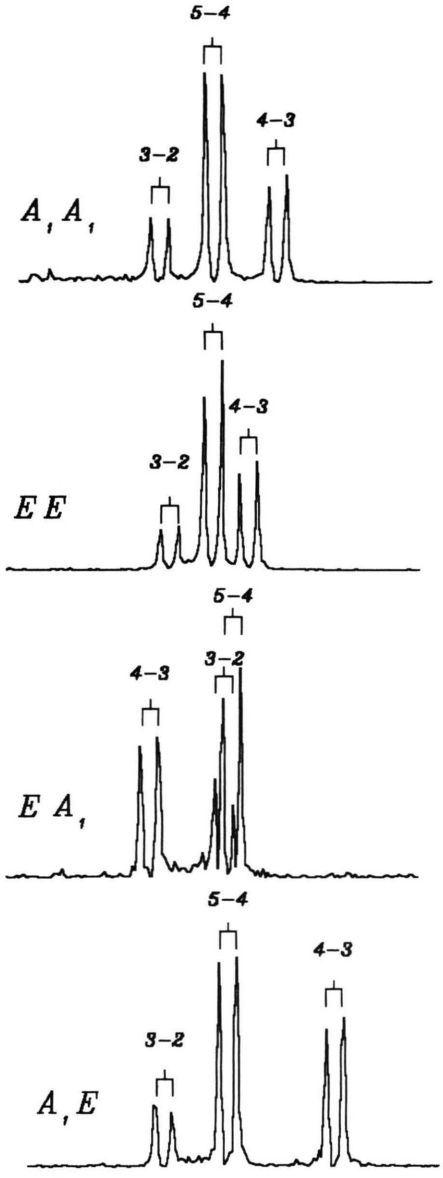

Fig. 2. The $4_{04}-3_{13}$ A_1A_1-, EA_1-, A_1E- and EE-species microwave transitions of 2,6-lutidine. The lines are split by nitrogen quadrupole coupling. The hyperfine components are additionally split by the Doppler effect.

val of 40 ns and 20 ns corresponding to a spectral resolution element of 3 and 6 kHz. The general set up of the spectrometer followed [2].

We used an automatic scan mode in the frequency range of 23.7 to 23.9 GHz and 26.1 to 26.5 GHz. In these regions we expected to find the $J_{K_-K_+} = 9_{19}-8_{08}$; $9_{09}-8_{18}$ and $10_{110}-9_{09}$; $10_{010}-9_{19}$ b-type-transition

Table 1. Observed rotational transitions of the A_1A_1 state of 2,6-lutidine. ν_{hfs} frequency of quadrupole components in MHz; δ_{hfs} observed-minus-calculated value in kHz.

J	K_-	K_+	$-J'$	K'_-	K'_+	$F-F'$	ν_{hfs}	δ_{hfs}
3	0	3	2	1	2	3 2	7 771.139	0.5
						2 1	7 770.184	0.1
						4 3	7 770.577	0.2
3	1	3	3	0	3	3 2	9 555.441	−0.7
						2 1	9 556.915	−1.0
						4 3	9 556.519	1.0
3	2	2	3	1	3	3 3	7 933.892	−0.3
						2 2	7 932.582	2.6
						4 4	7 932.919	−0.9
4	0	4	3	1	3	4 3	10 773.119	1.4
						3 2	10 772.833	−0.6
						5 4	10 772.963	−0.4
4	1	3	4	0	4	5 5	6 704.204	0.9
						3 3	6 703.663	−1.7
						4 4	6 706.300	0.3
4	1	4	3	0	3	4 3	11 739.340	−0.9
						3 2	11 740.169	−0.0
						5 4	11 740.029	0.3
4	3	1	4	2	2	3 3	8 454.553	−0.5
						4 4	8 453.057	−0.2
						5 5	8 454.248	0.7
5	0	5	4	1	4	5 4	13 553.698	−1.1
						4 3	13 553.667	−1.5
						6 5	13 553.723	0.8
5	1	5	4	0	4	5 4	14 007.199	−1.3
						4 3	14 007.626	−0.5
						6 5	14 007.590	−1.1
5	3	2	5	2	3	4 4	7 690.942	0.2
						5 5	7 689.956	−0.9
						6 6	7 690.773	−1.0
5	3	3	5	2	4	4 4	10 965.367	3.5
						5 5	10 965.736	0.2
						6 6	10 965.436	3.5
6	0	6	5	1	5	6 5	16 192.022	−2.3
						5 4	16 192.076	0.7
						7 6	16 192.106	2.0
6	1	6	5	0	5	6 5	16 384.860	6.1
						5 4	16 385.076	0.2
						7 6	16 385.076	−0.7
6	4	2	6	3	3	5 5	12 103.427	−0.5
						6 6	12 102.331	−0.1
						7 7	12 103.270	0.7
7	0	7	6	1	6	8 7	18 756.936	−1.2
						7 6	18 756.857	4.0
						6 5	18 756.916	−1.7
7	1	7	6	0	6	8 7	18 833.849	1.9
						7 6	18 833.709	1.0
						6 5	18 833.835	−1.2
7	2	5	7	1	6	6 6	10 035.919	0.5
						7 7	10 037.564	−0.5
						8 8	10 036.126	0.2
8	0	8	7	1	7	9 8	21 288.383	7.2
						8 7	21 288.293	−4.4
						7 6	21 288.358	−2.4
8	1	8	7	0	7	9 8	21 317.707	−0.3
						8 7	21 317.608	−2.4
						7 6	21 317.693	−1.8
9	0	9	8	1	8	10 9	23 805.904	2.5
						9 8	23 805.835	1.0
						8 7	23 805.887	−3.0
9	1	9	8	0	8	10 9	23 816.741	1.5
						9 8	23 816.668	1.9
						8 7	23 816.722	−4.0
10	0	10	9	1	9	11 10	26 317.946	0.9
						11 9	26 318.004	1.9
						9 8	26 317.987	−2.6
10	1	10	9	0	9	11 10	26 321.853	0.2
						10 9	26 321.914	2.5
						9 8	26 321.898	−2.1

Table 2. Observed rotational transitions of 2,6-lutidine. – ν_0 frequency of hyperfine free line, ν_R frequency of reference line, $\nu_R - \nu_{FF'}$ difference to reference line in MHz, $\delta(\nu_R - \nu_{FF'})$ observed-minus-calculated value in kHz.

J K_- K_+ F_R F'_R	J' K'_- K'_+ F F'	ν_0 ν_R $\nu_R - \nu_{FF'}$	$\delta(\nu_R - \nu_{FF'})$
A_1A_1-state			
3 0 3	2 1 2	7 770.691	
4 3		7 770.5772	
	2 1	0.3932	0.8
	3 2	−0.562	0.3
3 1 3	2 0 2	9 556.252	
4 3		9 556.5188	
	2 1	−0.396	−2.3
	3 2	1.0774	−1.0
3 2 2	3 1 3	7 933.163	
4 4		7 933.9189	
	2 2	0.3371	2.7
	3 3	−0.97325	2.2
4 0 4	3 1 3	10 772.989	
5 4		10 772.96315	
	3 2	0.13015	−0.3
	4 3	−0.15605	1.8
4 1 3	4 0 4	6 704.603	
5 5		6 704.204	
	4 4	−2.0954	−3.8
	3 3	0.5416	1.8
4 1 4	3 0 3	11 739.839	
5 4		11 740.0292	
	3 2	−0.1402	0.1
	4 3	0.6893	1.7
4 3 1	4 2 2	8 453.930	
5 5		8 453.24825	
	3 3	−0.3048	−1.2
	4 4	1.1909	−0.9
5 0 5	4 1 4	13 553.704	
5 4		13 553.6983	
	4 3	0.3125	−0.4
	6 5	−0.2435	1.9
5 1 5	4 0 4	14 007.474	
6 5		14 007.58955	
	4 3	−0.3655	0.6
	5 4	0.39095	−0.3
5 3 2	5 2 3	7 690.547	
6 6		7 690.7734	
	4 4	−0.16825	1.2
	5 5	0.8184	1.7
5 3 3	5 2 4	10 965.517	
6 6		10 965.4364	
	4 4	0.06945	−7.9
	5 5	−0.2993	−2.7
6 0 6	5 1 5	16 192.073	
5 4		16 192.0762	
	6 5	0.54	−4.6
	7 6	−0.2995	1.1
6 1 6	5 0 5	16 385.006	
7 6		16 385.07635	
	5 4	0.0	0.5
	6 5	0.2215	−1.3
6 4 2	6 3 3	12 103.001	
7 7		12 103.26955	
	5 5	−0.15715	−1.2
	6 6	0.93875	−0.8
7 0 7	6 1 6	18 756.910	
6 5		18 756.9191	
	7 6	0.0619	−5.5
	8 7	−0.0195	−0.5
7 1 7	6 0 6	18 833.802	
6 5		18 833.8345	
	7 6	0.1256	3.9
	8 7	−0.0147	3.4
7 2 5	7 1 6	10 036.543	
8 8		10 036.1259	
	6 6	0.2072	0.5
	7 7	1.4376	−0.4
8 0 8	7 0 7	21 288.350	
7 6		21 288.3577	
	8 7	0.0651	−2.0
	9 8	−0.0258	−9.7
8 1 8	7 1 7	21 317.677	
7 6		21 317.6922	
	8 7	0.0842	−0.7
	9 8	−0.0151	1.5
9 0 9	8 1 8	23 805.882	
8 7		23 805.8847	
	9 8	0.0498	3.9
	10 9	−0.0193	5.4
9 1 9	8 0 8	23 816.718	
8 7		23 816.722	
	9 8	0.0547	5.8
	10 9	−0.0186	5.5
10 0 10	9 1 9	26 317.989	
9 8		26 317.9874	
	10 9	0.0413	3.4
	11 10	−0.0166	4.4
10 1 10	9 0 9	26 321.898	
9 8		26 321.8977	
	10 9	0.04475	2.2
	11 10	−0.0165	4.6
A_1E-state			
4 0 4	3 1 3	10 637.324	
5 4		10 637.278	
	3 2	0.15545	−0.1
	4 3	−0.26235	−1.5
5 0 5	4 1 4	13 480.719	
6 5		13 480.72945	
	4 3	0.066	5.6
	5 4	−0.02255	−2.7
5 1 5	4 0 4	14 068.978	
6 5		14 069.11725	
	5 4	0.4877	−0.7
	4 3	−0.06705	−4.9
7 0 7	6 1 6	18 732.928	
6 5		18 732.9421	
	7 6	0.0653	2.1
	8 7	−0.0202	0.7
8 0 8	7 1 7	21 270.332	
7 6		21 270.3443	
	8 7	0.0633	2.8
	9 8	−0.0224	6.9

Table 2 (continued)

J K_- K_+ F_R F'_R	J' K'_- K'_+ F F'	ν_0 ν_R $\nu_R-\nu_{FF'}$	$\delta(\nu_R-\nu_{FF'})$
EA_1-state			
4 0 4	3 1 3	11 182.131	
3 2		11 182.2205	
	4 3	0.1815	2.4
	5 4	−0.01795	−2.9
4 1 4	3 0 3	11 375.524	
5 4		11 375.6549	
	3 2	−0.0718	1.1
	4 3	0.4556	5.5
5 0 5	4 1 4	13 728.348	
4 3		13 728.3859	
	5 4	0.14415	−1.2
	6 5	−0.02355	4.8
7 0 7	6 1 6	18 772.549	
6 5		18 772.571	
	7 6	0.09	−0.3
	8 7	−0.021	4.1
7 1 7	6 0 6	18 787.793	
6 5		18 787.8194	
	7 6	0.1036	1.9
	8 7	−0.0202	5.5
8 1 8	7 0 7	21 290.332	
7 6		21 290.3397	
	8 7	0.0754	0.3
	9 8	−0.0208	6.1
9 0 9	8 1 8	23 796.659	
8 7		23 796.6714	
	9 8	0.0583	−2.1
	10 9	−0.0181	4.5
9 1 9	8 0 8	23 794.544	
8 7		23 794.55645	
	9 8	0.05625	1.5
	10 9	−0.0163	2.9
EE-state			
3 2 2	3 1 3	7 933.614	
4 4		7 933.919	
	3 3	−1.3452	−1.7
	2 2	0.4717	−0.3
3 0 3	2 1 2	7 955.582	
4 3		7 955.5314	
	2 1	0.2659	−0.9
	3 2	−0.3452	2.7
3 1 3	2 0 2	9 442.429	
4 3		9 442.6426	
	3 2	1.0288	−1.9
	2 1	−0.3867	−1.1
4 0 4	3 1 3	10 843.536	
5 4		10 843.5348	
	3 2	0.1043	−0.8
	4 3	−0.08625	−1.3
4 1 4	3 0 3	11 685.979	
5 4		11 686.1596	
	3 2	0.6854	−1.2
	4 3	−0.1424	0.2
4 1 3	4 0 4	6 772.615	
5 5		6 772.0919	
	3 3	0.507	6.8
	4 4	−2.0009	2.8
5 0 5	4 1 4	13 578.346	
6 5		13 578.3785	
	4 3	0.0543	−7.8
	5 4	0.0543	−7.7
5 1 5	4 0 4	13 978.842	
6 5		13 978.9607	
	4 3	−0.0351	−1.5
	5 4	0.3904	−0.3
5 1 4	5 0 5	9 308.394	
6 6		9 307.85385	
	4 4	0.40425	−1.6
	5 5	−1.97835	3.2
6 1 6	5 0 5	16 368.333	
6 5		16 368.1645	
	5 4	−0.222	0.0
	7 6	−0.222	−0.1
7 0 7	6 1 6	18 754.707	
6 5		18 754.6914	
	7 6	−0.0.695	6.1
	8 7	0.02415	4.0
7 1 7	6 0 6	18 822.566	
6 5		18 822.6173	
	7 6	0.12625	2.2
	8 7	−0.01375	2.3
7 2 5	7 1 6	10 129.232	
8 8		10 129.6198	
	6 6	−0.1963	0.0
	7 7	1.3593	1.7
8 0 8	7 1 7	21 282.881	
7 6		22 288.8962	
	8 7	0.0701	−4.7
	9 8	−0.0201	5.3
8 1 8	7 0 7	21 308.705	
7 6		21 308.7287	
	8 7	0.08545	−1.0
	9 8	−0.0154	1.9
9 0 9	8 1 8	23 799.0908	
8 7		23 805.10255	
	9 8	0.0538	1.3
	10 9	−0.01525	1.6
9 1 9	8 0 8	23 808.605	
8 7		23 808.6351	
	9 8	0.05985	1.5
	10 9	−0.01515	2.2
10 0 10	9 1 9	26 310.667	
9 8		26 310.6746	
	10 9	0.0444	1.2
	11 10	−0.016	4.4
10 1 10	9 0 9	26 314.089	
9 8		26 314.0986	
	10 9	0.0412	6.0
	11 10	0.0174	5.5

Table 3. Hyperfine free transitions of the $\sigma_i\,\sigma_j = A_1E$, EA_1 and EE states of 2,6-lutidine, and the difference to the A_1A_1 lines derived from Table 2. $\nu(\sigma_i\,\sigma_j)$ frequency of $\sigma_i\,\sigma_j$ state line, $\Delta\nu$ splitting between the A_1A_1 line and the A_1E, EA_1 or EE line in MHz, and $\delta\nu$ observed-minus-calculated for $\Delta\nu$ in MHz.

Transition		$\sigma_i\,\sigma_j$	$\nu(\sigma_i\,\sigma_j)$	$\Delta\nu$	$\delta\nu$
3 0 3	2 1 2	EE	7 955.582	−184.891	0.943
3 1 3	2 0 2	EE	9 442.429	113.609	−0.512
3 2 2	3 1 3	EE	6 889.013	1044.150	−4.896
4 0 4	3 1 3	A_1E	10 637.324	135.665	1.023
		EA_1	11 182.131	−409.142	−5.863
		EE	10 843.536	−70.547	0.127
4 1 4	3 0 3	EA_1	11 375.524	364.315	5.503
		EE	11 685.979	53.860	0.047
4 1 3	4 0 4	EE	6 772.615	68.012	0.322
5 0 5	4 1 4	A_1E	13 480.719	72.985	0.364
		EA_1	13 728.348	−174.644	−2.830
		EE	13 578.346	−24.642	−0.118
5 1 5	4 0 4	A_1E	14 068.978	−61.504	−0.804
		EE	13 978.842	28.632	0.061
5 1 4	5 0 5	EE	9 308.394	28.012	0.322
6 1 6	5 0 5	EE	16 368.233	16.673	−0.041
7 0 7	6 1 6	A_1E	18 732.928	23.991	−0.208
		EA_1	18 772.549	−15.630	−0.749
		EE	18 754.707	2.212	−0.218
7 1 7	6 0 6	EA_1	18 787.793	46.009	0.180
		EE	18 822.566	11.236	−0.141
7 2 5	7 1 6	EE	10 129.232	−92.689	1.021
8 0 8	7 1 7	A_1E	21 270.332	18.018	−0.347
		EE	21 282.881	5.469	−0.261
8 1 8	7 0 7	EA_1	21 290.332	27.345	−0.210
		EE	21 308.705	8.972	−0.225
9 0 9	8 1 8	EA_1	23 794.544	9.223	−0.548
		EE	23 799.091	6.791	−0.302
9 1 9	8 0 8	EA_1	23 796.659	−20.060	−0.407
		EE	23 808.605	8.113	−0.276
10 0 10	9 1 9	EE	26 310.667	7.322	−0.345
10 1 10	9 0 9	EE	26 314.089	7.809	−0.346

of the A_1A_1, A_1E, EA_1 and EE substates. Using these four A_1A_1 transitions we could predict the other A_1A_1 rotational transitions.

We assigned 23 A_1A_1, 5 A_1E, 8 EA_1, and 19 EE transitions. For all measurements we used a mixture of 1 to 2% of LUT in argon, at a pressure of 40 kPa (0.4 atm). The substance was purchased from Aldrich Chemie GmbH, Steinheim, FRG.

The measured transitions are given in the Tables 1, 2, and 3. The frequencies are given as the mean values of the Doppler doublets.

Theory and Analysis

The rotational spectrum of LUT was analysed using a semi rigid rotor model including centrifugal distortion and internal rotation of two methyl groups. Three degrees of freedom arise from the overall and two from the internal rotation. The frame and the two methyl tops were assumed to be quasi rigid but centrifugally distorted. The internal rotation theory of two top molecules was given for the time by Swalen and Costain [3]. The general internal rotation theory was reviewed by Lin and Swalen [4] and by Dreizler [5].

The Hamiltonian for molecules with C_{2v} symmetry and a xz-plane of symmetry containing the internal rotor axes may be written as

$$H = B_x P_x^2 + B_y P_y^2 + B_z P_z^2 \qquad H_R \quad (1\,a)$$

$$+ 2Q_x P_x (p_1 + p_2) + 2Q_z P_z (p_1 - p_2) \qquad H_{RT} \quad (1\,b)$$

$$+ \sum_{i=1}^{2} F p_i^2 + \tfrac{1}{2} V_3 (1 - \cos 3\alpha_i) \qquad H_1, H_2 \quad (1\,c)$$

with I^r-representation, $x = b$, $y = c$ and $z = a$, which is used in Figure 1.

$$B_x = \frac{\hbar^2}{2I_x} + 2F\varrho_x^2, \tag{2a}$$

$$B_y = \frac{\hbar^2}{2I_y}, \tag{2b}$$

$$B_z = \frac{\hbar^2}{2I_z} + 2F\varrho_z^2, \tag{2c}$$

P_g = components of total angular momentum operator, $g = x, y, z$

$$Q_g = F\varrho_g, \quad g = x, z, \tag{3}$$

$$F = \frac{\hbar^2}{4I_\alpha}\frac{1}{r}, \tag{4}$$

$$r = 1 - \frac{\lambda_x^2 I_\alpha}{I_x} - \frac{\lambda_z^2 I_\alpha}{I_z}, \tag{5}$$

$$\varrho_g = \frac{\lambda_g I_\alpha}{I_g}, \tag{6}$$

p_i = total angular momentum of the methyl top i about its symmetry axis, $i = 1, 2$;
I_g = moments of inertia of the molecule with frozen internal rotation, $g = x, y, z$;
I_α = moment of inertia of the methyl top;
λ_g = direction cosine between g- and internal rotator axis;
α_i = internal rotation angle, $i = 1, 2$;
V_3 = potential barrier.

Terms in $p_1 p_2$ have been neglect. The interaction terms V_{12}, V'_{12}, and V_6 cannot be determined from the torsional ground state alone. Therefore they were set to zero.

The Hamiltonian (1) is invariant under the group $C_{3v}^- \otimes C_{3v}^+$ [6, 7]. The rotational lines split into quartets labelled by the symmetry species A_1A_1, A_1E, EA_1, and EE.

Due to ^{14}N quadrupole coupling each component of the torsional multiplet shows a small additional splitting. We could determine the hyperfine free lines using the method given in [8]. The hyperfine free A_1A_1–A_1E, A_1A_1–EA_1, and A_1A_1–EE splittings are given in Table 3. A low V_3 barrier can be determined from the inertial defect of the A_1A_1 spectrum alone [1]. Next we describe the method for a two top molecule with a planar x,z-frame and the internal rotation axes in the plane, that is $\lambda_y = 0$. We neglect the centrifugal distortion. Using perturbation theory an effective rotational Hamiltonian may be derived from (1) [9].

$$H_{v_1\sigma_1 v_2\sigma_2} = \frac{\hbar^2}{2I_x} P_x^2 + \frac{\hbar^2}{2I_y} P_y^2 + \frac{\hbar^2}{2I_z} P_z^2 \tag{7a}$$

$$+ F \sum_{n=1}^{2} \left(W^{(n)}_{v_1\sigma_1} \mathscr{P}_1^n + W^{(n)}_{v_1\sigma_2} \mathscr{P}_2^n\right) \tag{7b}$$

with $\mathscr{P}_i = \varrho_{xi} P_x + \varrho_{zi} P_z$ for two tops $i = 1, 2$. σ_i describes the species [4]. $W^{(n)}_{v\sigma}$ is the perturbation coefficient resulting from a van Vleck transformation [10]. It is a function of the reduced barrier

$$s = \frac{4}{9} \frac{V_3}{F}. \tag{8}$$

For the A_1A_1-state (7) reduces to

$$H_{0000} = \sum_{g=x,y,z} \frac{\hbar^2}{2I_g} P_g^2 + 2FW_{00}^{(2)} (\varrho_x^2 P_x^2 + \varrho_z^2 P_z^2). \tag{9}$$

In (9) modified rotational constants $\overline{B_g}$ may be introduced. To this order of perturbation the spectrum should be that of a quasi-rigid asymmetric top.

$$\overline{B_x} = \frac{\hbar^2}{2I_x} + 2FW_{00}^{(2)} \varrho_x^2,$$

$$\overline{B_y} = B_y = \frac{\hbar^2}{2I_y}, \tag{10}$$

$$\overline{B_z} = \frac{\hbar^2}{2I_z} + 2FW_{00}^{(2)} \varrho_z^2,$$

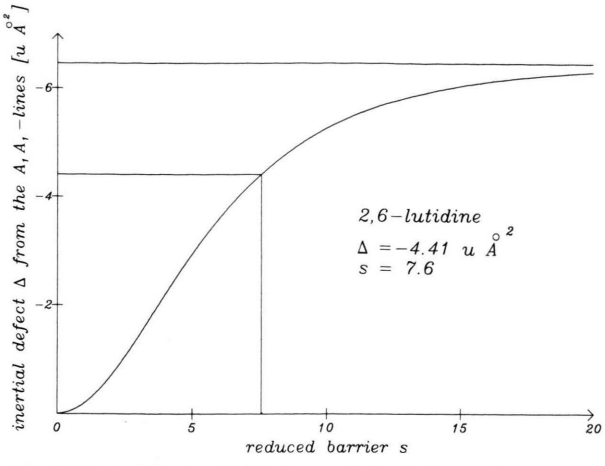

Fig. 3. Plot of the inertial defect Δ of the A_1A_1-species versus the reduced barrier s.

$\overline{B_y}$ is unchanged as the internal rotation axes are in the xz-plane. For infinite barriers $W_{00}^{(2)}$ vanishes and the rotational constants converge to the value of a molecule with frozen internal rotation. For zero barrier ($s = 0$) $W_{00}^{(2)} = 1$ (see appendix) the rotational constants become

$$\overline{B_x^0} = \frac{\hbar^2}{2I_x} + 2F\varrho_x^2 = B_x,$$

$$\overline{B_y^0} = \frac{\hbar^2}{2I_y} = B_y, \tag{11}$$

$$\overline{B_z^0} = \frac{\hbar^2}{2I_z} + 2F\varrho_z^2 = B_z.$$

In the appendix it is shown, that the inertial defect Δ for vanishing barrier $s = 0$ is:

$$\Delta = \frac{\hbar^2}{2} \left(\frac{1}{\overline{B_y^0}} - \frac{1}{\overline{B_x^0}} - \frac{1}{\overline{B_z^0}} \right) = 0. \tag{12}$$

In Fig. 3 the inertial defect derived from the $\overline{B_g}$ constants of (10) is drawn as a function of the reduced barrier s. The effective inertial defect is -4.41 uÅ^2, which is about 2 uÅ^2 smaller (absolute value) than those given in Table V in [11]. Using the A_1A_1 rotational constants (see below) of Table 4 a value of $s = 7.6$ can be determined.

For the analysis of internal rotation splittings the principal axis method (PAM) was used as outlined by Meyer and Dreizler [12]. The program TTWF2 [13] diagonalizes a sufficient part of the rotation internal-rotation Hamiltonian matrix.

Table 4. Rotational, centrifugal distortion (Watson's A-reduction [22]), quadrupole coupling constants, standard deviation, inertial defect, reduced barrier, and barrier of 2,6-lutidine derived from the inertia defect of the A_1A_1 spectrum.

A	(MHz)	3540.57930 (40)
B	(MHz)	1910.90321 (34)
C	(MHz)	1254.65947 (13)
Δ_J	(kHz)	0.0977 (60)
Δ_{JK}	(kHz)	0.9849 (293)
Δ_K	(kHz)	2.9060 (516)
δ_J	(kHz)	0.0386 (23)
δ_K	(kHz)	0.6539 (666)
χ_{aa}	(MHz)	1.599 (5)
χ_{bb}	(MHz)	−4.572 (5)
χ_{cc}	(MHz)	2.973 (5)
σ	(kHz)	2.2
Δ_{AA}	(uÅ^2)	−4.41
s		7.6
V_3	(kJ/mol)	1.085
V_3	(cal/mol)	259.32

Table 5. Rotational, centrifugal distortion constants (Watson's A-reduction [23]), potential barrier, angle between x- and z-axis and internal rotation axis (α_x, α_z) of 2,6-lutidine from MW-spectrum and from ab initio calculation with Gaussian-90 using the basis set 6-311G**.

		MW-spectrum	6-311G**
A	(MHz)	3509.7139 (84)	3587.275
B	(MHz)	1906.8639 (101)	1918.044
C	(MHz)	1254.6215 (14)	1269.369
D_J	(kHz)	0.0638 (1)	–
D_{JK}	(kHz)	−0.2493 (3)	–
D_K	(kHz)	1.2565 (47)	–
δ_J	(kHz)	0.0193 (4)	–
δ_K	(kHz)	0.2268 (333)	–
V_3	(kJ/mol)	1.1752 (32)	1.2445 (8)
V_6	(kJ/mol)	–	0.0196 (15)
V_{12}	(kJ/mol)	–	0.0630 (7)
V'_{12}	(kJ/mol)	–	0.0059 (26)
I_α	(uÅ^2)	3.0808 (9)	3.093
α_x	(°)	33.803 (11)	32.55
α_z	(°)	56.197 (11)	57.45

From the splittings (Table 3) we calculated not only the reduced barrier s but also I_α and the angles (α_x, α_z) between the internal rotation axis and the x- and z-axis (Table 5).

The potential barrier obtained from the A_1A_1–EE, A_1A_1–A_1E, and A_1A_1–EA_1 splittings is 1.1752 kJ/mol (280.88 cal/mol), the calculated value from the inertial defect is 1.085 kJ/mol (259.32 cal/mol).

Ab initio Calculation

The rotational constants were calculated with the Gaussian 90 program [14]. The basis set 6-311G** [15] was used for structure optimizations. The calculated rotational constants are approx. 0.5 (C-constant) to 2.0 percent (A-constant) too large. The calculated angle between the internal rotations axis and the principal inertia axis deviates about 2 percent from the measured one (Table 5).

The barrier hight to internal rotation was calculated by a method similar to that given by Alijibury [16].

The torsional potential function for molecules with two methyl groups is

$$V(\alpha_1, \alpha_2) = \tfrac{1}{2} V_3(1-\cos 3\alpha_1) + \tfrac{1}{2} V_3(1-\cos 3\alpha_2) + \tfrac{1}{2} V_6(1-\cos 6\alpha_1) + \tfrac{1}{2} V_6(1-\cos \alpha_2) + V_{12}(\cos 3\alpha_1 \cos 3\alpha_2 - 1) + V_{12} \sin 3\alpha_3 \sin 3\alpha_2 + \ldots . \quad (13)$$

For the ab initio calculation we considered all terms including the V_6, V_{12}, and V'_{12}.

The torsional angle α_1 referring to one methyl group of LUT was described by the dihedral angle of the plane H3C7C1 and C7C1N. H1 (and H7) is the in-plane hydrogen atom of the equilibrium structure with $\alpha_1 = \alpha_2 = 0°$. First, this structure was optimized employing the 6-311 G** basis set. Then we calculated with this structure for different values of the torsion angles α_1 and α_2 the energy increment $\delta E(\alpha_1, \alpha_2) = E(\alpha_1, \alpha_2) - E(0°, 0°)$. The V_3, V_6, V_{12}, and V'_{12} potential barrier coefficient were fitted to the energy increment function δE. The experimental and calculated potential terms are listed in Table 5.

Quadrupole Coupling

Prior to the internal rotation analysis, the ^{14}N quadrupole coupling, rotational constants, and centrifugal distortion from the A_1A_1 species lines were evaluated. Here first order perturbation theory according to [17] was sufficient. The program HFS written by Gripp was used [18]. The results are given in Table 4. This analysis provided also the hyperfine free center frequencies ν_0 of the hyperfine multiplets.

Table 6. Quadrupole coupling constants of 2,6-lutidine determined from the transitions of A_1A_1 state alone and from a combined analysis of transitions of all torsional states given in Table 3, σ standard deviation. For comparison the quadrupole coupling constants of pyridin [22] are given.

		A_1A_1-state	A_1A_1-, EE-, A_1E-, and EA_1-state	Pyridine
χ_{zz}	(MHz)	1.599 (5)	1.600 (5)	1.434 (3)
χ_{xx}	(MHz)	−4.572 (5)	−4.572 (5)	−4.908 (3)
χ_{yy}	(MHz)	2.973 (5)	2.972 (3)	3.474 (3)
σ	(kHz)	2.2	3.5	

Nuclear hyperfine structure of the A_1A_1, A_1E, EA_1, and EE-species were analysed using first order perturbation theory.

$$E_{\sigma_{J_{K_-K_+}}} = \frac{2}{J(J+1)} (\chi_{aa}\langle P_{a\sigma}^2\rangle + \chi_{bb}\langle P_{b\sigma}^2\rangle + \chi_{cc}\langle P_{c\sigma}^2\rangle) . \tag{14}$$

Because of the C_{2v} symmetry of LUT the off-diagonal elements of the nitrogen quadrupole coupling tensor χ vanish. The splitting of the hyperfine structure depends on the torsional sublevel as obvious from Figure 2. In contrast to the analysis of the A_1A_1 spectrum we analysed only the hyperfine splitting.

We calculated the $\langle P_{g\sigma}^2\rangle$ with the Hellmann-Feynman theorem [19] and the Hamiltonian (1).

$$\langle P_{g\sigma}^2\rangle = \left\langle \frac{\partial H}{\partial B_g} \right\rangle = \frac{dE_{J_{K_-K_+}}}{dB_g} \approx \frac{E_{J_{K_-K_+}}(B_g + \Delta B_g) - E_{J_{K_-K_+}}(B_g)}{\Delta B_g} , \tag{15}$$

were B_g are the rotational constants and $\Delta B_g/B_g$ is 10^{-3}. The result is given in Table 6. So we analysed the quadrupole coupling and the internal rotation consecutively. The quadrupole coupling constants are similar, but not equal to those of pyridine.

Conclusion

We measured and assigned the rotational spectrum of LUT in its vibrational and torsional ground state. From the inertial defect of the A_1A_1-lines and from the splittings between the A_1A_1–EA_1, A_1A_1–A_1E, and A_1A_1–EE components of a rotational transition we were able to determine the potential barrier V_3. We have shown that the potential barrier can be successfully obtained from the inertial defect especially in the case of small potential barriers. We could determine the nitrogen quadrupole coupling tensor from the A_1A_1 species components using a quasi-rigid model and also from all other species using an internal rotational model. The value for the quadrupole coupling constants resulting from both methods are equal.

Appendix

For the reduced barrier $s = 0$ the eigenfunction $U_{v\sigma}(\alpha)$ of the internal rotation Hamiltonian for one top contained in (1c) approaches

$$U_{v\sigma}(\alpha) \to U_m(\alpha) = \frac{1}{\sqrt{2\pi}} e^{im\alpha} . \tag{A.1}$$

In our case $v\sigma = 00$ is correlated to $m=0$. m is the quantum number of free internal rotation [20]. The perturbation coefficient $W_{v\sigma}^{(2)}$ is defined as

$$W_{v\sigma}^{(2)} = 1 + \frac{16}{9} \sum_{v \neq v'} \frac{|\langle v\sigma | p | v'\sigma'\rangle|^2}{b_{v\sigma} - b_{v'\sigma'}} \tag{A.2}$$

with the internal rotation operator

$$p = -i \frac{\partial}{\partial \alpha} \tag{A.3}$$

and

$$b_{v\sigma} = \frac{4E_{v\sigma}}{9F} . \tag{A.4}$$

$E_{v\sigma}$ and $b_{v\sigma}$ are Mathieu- and reduced Mathieu eigenvalues. For $v' \neq v$ or $m' \neq m$ the matrix elements $\langle v\sigma | p | v'\sigma'\rangle = 0$ for $s = 0$. Therefore

$$W_{v\sigma}^{(2)}(0) = 1 . \tag{A.5}$$

From (10) the modified moment of inertia $\overline{I_x}$ for a zero barrier two top molecule is

$$\frac{\hbar^2}{2\overline{B}_x} = \overline{I}_x = \frac{1}{\frac{1}{I_x} + \frac{2\lambda_x^2 I_\alpha}{r I_x^2}} \tag{A.6}$$

or

$$\overline{I}_x = \frac{r I_x}{r + \frac{2\lambda_x^2 I_\alpha}{I_x}} \tag{A.7}$$

with

$$\frac{\lambda_g^2 I_\alpha}{I_g} \ll 1 \tag{A.8a}$$

and

$$r \approx 1 \tag{A.8b}$$

which are reasonably fulfilled, it approximately results

$$\overline{I_x} = I_x\left(1 - \frac{2\lambda_x^2 I_\alpha}{I_x}\right) \tag{A.9a}$$

and similar

$$\overline{I_z} = I_z\left(1 - \frac{2\lambda_z^2 I_\alpha}{I_z}\right) \tag{A.9b}$$

but

$$\overline{I_y} = I_y\,. \tag{A.9c}$$

The inertial defect Δ for a molecule with the internal rotation axis in the xz-plane is

$$\Delta = \overline{I_y} - \overline{I_x} - \overline{I_z} = I_y - (I_x - 2\lambda_x^2 I_\alpha) - (I_z - 2\lambda_z^2 I_\alpha)\,. \tag{A.10}$$

For a one top molecule Δ with $\lambda_x = 0$, $\lambda_z = 1$ reduced to

$$\Delta = I_y - I_x - (I_z - I_\alpha) \tag{A.11}$$

which is well known [21].

From (A.10) it follows

$$\Delta = I_y - (I_x + I_z - 2I_\alpha)\,. \tag{A.12}$$

As for a molecule with a planar frame and two C_{3v} symmetric tops

$$I_y - I_x - I_z = 2I_\alpha \tag{A.13}$$

it results from (A.10) and (A.13) for the inertial defect

$$\Delta = 0\,. \tag{A.14}$$

The inertial defect for a semi-rigid molecule with a planar frame and two (or one) tops vanishes in good approximation for the zero barrier limit. Other vibrational effects are neglected by the semi-rigid model.

Acknowledgement

We thank the members of our group for help and discussion. Financial support from the Bundesministerium für Forschung und Technologie, Funds of the Deutsche Forschungsgemeinschaft, Fonds der Chemie, and the Land Schleswig-Holstein are gratefully acknowledged. The calculations were carried out at the computer centre of the University of Kiel.

[1] W. Caminati and S. Di Bernardo, Chem. Phys. Lett. **171,** 39 (1990).
[2] U. Andresen, H. Dreizler, J.-U. Grabow, and W. Stahl, Rev. Sci. Instrum. **61,** 3694 (1990).
[3] J. D. Swalen and C. C. Costain, J. Chem. Phys. **31,** 1562 (1959).
[4] C. C. Lin and J. D. Swalen, Rev. Mod. Phys. **31,** 841 (1959).
[5] H. Dreizler, Fortschr. Che. Forschung **10,** 59 (1968).
[6] R. M. Myers and E. Br. Wilson jr., J. Chem. Phys. **33,** 186 (1960).
[7] loc. cit. [5], Chapter 5.
[8] H. R. Rudolph, Z. Naturforsch. **23a,** 540 (1968).
[9] Loc. cit. [5], Eq. 10.4.
[10] D. R. Herschbach, J. Chem. Phys. **31,** 91 (1959).
[11] J. Demaison, D. Schwoch, B. T. Tan, and H. D. Rudolph, J. Mol. Spectrosc. **83,** 391 (1980).
[12] M. Meyer and H. Dreizler, J. Mol. Spectrosc. **148,** 310 (1991).
[13] M. Meyer, Thesis, Kiel 1990.
[14] M. J. Frisch, M. Head-Gordon, G. W. Trucks, J. B. Foresman, H. B. Schlegel, R. Raghavachari, M. Robb, J. S. Brinkley, C. Gonzales, D. J. De Frees, D. J. Fox, R. A. Whiteside, R. Seeger, C. F. Melius, J. Baker, R. L. Martin, L. R. Kahn, J. J. P. Stewart, E. W. Fluder, S. Topiol, and J. A. Pople, Gaussian Inc., Pittsburgh, PA 1990.
[15] R. Krishnan, J. S. Brinkley, R. Seeger, and J. A. Pople, J. Chem. Phys. **72,** 650 (1980).
[16] A. L. Aljinbury, R. G. Snyder, H. L. Strauss, and K. Raghavachari, J. Chem. Phys. **84,** 6872 (1986).
[17] W. Gordy and R. L. Cook, Microwave Molecular Spectra, J. Wiley, New York 1984, Chapt. IX.4.
[18] J. Gripp, HFS-Program, Kiel 1989.
[19] P. W. Atkins, Molecular Quantum Mechanics, Oxford University Press, Oxford, New York 1983, Eq. 8.4.1.
[20] loc. cit. [5], Eq. 7.39.
[21] E. Br. Wilson jr., C. C. Lin, and D. R. Lide jr., J. Chem. Phys. **23,** 136 (1955).
[22] N. Heineking, H. Dreizler, and R. Schwarz, Z. Naturforsch. **41a,** 1210 (1986).
[23] J. K. G. Watson, J. Chem. Phys. **46,** 1935 (1967).